Journal of Constructional Steel Research 99 (2014) 187–193

Contents lists available at ScienceDirect

Journal of Constructional Steel Research

Shape optimization design of steel shear panel dampers

Kailai Deng [a], Peng Pan [b,*], Jiangbo Sun [a], Jixin Liu [a], Yantao Xue [c]

[a] Department of Civil Engineering, Tsinghua University, Beijing 100084, China
[b] Key Laboratory of Civil Engineering Safety and Durability of China Education Ministry, Department of Civil Engineering, Tsinghua University, Beijing 100084, China
[c] Institute of Building Structures, China Academy of Building Research, Beijing 100013, China

ARTICLE INFO

Article history:
Received 10 December 2013
Accepted 3 March 2014
Available online 15 May 2014

Keywords:
Steel shear panel damper
Shape optimization
Simulating annealing
Finite element analysis
Low cycle fatigue performance

ABSTRACT

Steel shear panel dampers (SSPDs) have a reasonably good and stable energy dissipation capacity, and are widely used in engineering to enhance the structural safety of buildings in large earthquakes. Efforts to improve the low cycle fatigue performance of SSPDs have focused mostly on the arrangement of the stiffeners or on the effects of the material properties. The shape of the SSPD plate has not been well investigated. This paper presents a shape optimization method for improving the low cycle fatigue performance of SSPDs. The shear plate shape of the SSPD is taken as the variable in the optimization process. The low cycle fatigue performance of the SSPD is assumed to have a negative relationship to the maximum equivalent plastic strain in the cyclic loading process. The equivalent plastic strains are obtained using the finite element software ABAQUS. The simulated annealing method is adopted for the optimization, which is capable of solving optimization problems involving strong nonlinear systems. In the optimization, four types of SSPDs with different aspect were modeled and the optimal shape of the SSPD for each case was derived. It can be found that the low cycle fatigue performance of the SSPD was significantly improved and the global optimal solution showed better performance compared to the local optimal solution.

1. Introduction

Steel shear panel dampers (SSPDs) have good energy dissipation capacity under cyclic loading. In recent decades, studies have shown the effectiveness of SSPDs in reducing the response of structures to earthquake ground motion [1–4]. As shown in Fig. 1(a), An SSPD consists of a steel shear plate and stiffeners. Considerable effort has been made to improve the low cycle fatigue performance of SSPDs; however, most researchers have focused on the arrangement of the stiffeners and the effects of the steel properties while the shape of SSPDs has not been well investigated. Low cycle fatigue damage in SSPDs commonly occurs at the weld heat-affected zones that are subjected to cyclic loading [5]. As shown in Fig. 1(b), a low cycle fatigue crack appeared at the left side of the middle zone of the SSPD, where the low cycle fatigue capacity of the steel is significantly weakened because of the weld between the steel plate and the stiffener [6,7]. Therefore, removing the weld heat-affected zone would improve the fatigue strength qualities of the SSPD.

Zhang et al. carried out physical tests on different structures of SSPDs [8]. They tested the thickness and shape of the steel shear plate and showed that the shear panel with its center weakened presented satisfactory deformation capacity and low cycle fatigue performance. Liu et al. changed the shape of the steel shear plate of the SSPDs and conducted quasi-static tests to investigate their performance [9]. They found that an arc-shaped SPD had better deformation capacity than SSPDs with stiffeners. In subsequent studies, Liu and Shimoda built a numerical model of the SSPD in ABAQUS and conducted a shape optimization process [10] where the side edges of the SSPD are assumed to be a parabola. The parameters of the parabola are taken as the variables and the maximum equivalent plastic strain (EPS) under a prescribed cyclic loading scheme is taken as the objective in the optimization. The response surface method is used and the optimal parameter of each optimization level is derived by regression analysis. After the optimization process, the maximum EPS of the SSPD was significantly reduced while the total dissipated energy capacity was similar to that of the initial model. The optimal parameters in each iteration were obtained by regression analysis. In the study of Liu et al., only the optimal shape of SSPDs with a square web was derived while the optimal shape for SSPD with a rectangular web was not investigated. In addition, since the edges of the SSPD are assumed to be a parabola, optimal shape derived was not necessarily a global optimal solution but a local optimal solution.

With the development of computer technology, more and more optimization algorithms are being applied in structural optimization; these include the simulated annealing (SA) algorithm, genetic algorithm (GA), and multi-level multi-disciplinary optimization methods (MDO), [11–15]. Ohsaki et al. adopted the SA algorithm to obtain the

* Corresponding author. Tel.: +86 10 62794729; fax: +86 10 62788620.
E-mail address: panpeng@mail.tsinghua.edu.cn (P. Pan).

http://dx.doi.org/10.1016/j.jcsr.2014.03.001
0143-974X/

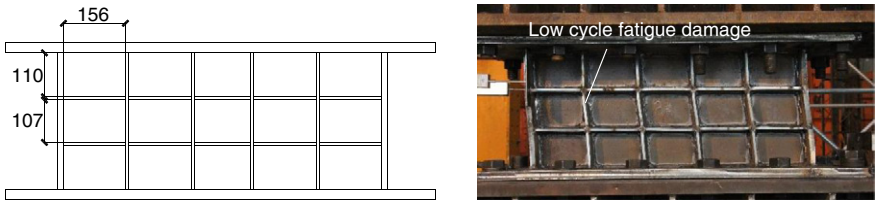

(a) Details of SSPD (b) Damage pattern of SSPD

Fig. 1. Details of SSPD and SSPD showing fatigue damage.

optimal amount and position of a stiffener in a steel link to improve the low cycle fatigue performance of steel links [16]. The results showed a significant improvement in the low cycle fatigue performance of the optimized steel link, demonstrating the effectiveness of the SA algorithm.

This paper presents a shape optimization method that uses the simulated annealing method to improve the low cycle fatigue performance of SSPDs. The shear plate shape of the SSPD is taken as the variable in the optimization process. The low cycle fatigue performance of the SSPDs is assumed to have a negative relationship with the maximum equivalent plastic strain in a cyclic loading process. The equivalent plastic strains are obtained using the finite element software ABAQUS. Optimization was performed on four types of SSPDs with different aspect ratios and the optimal shapes of the SSPDs were derived.

2. Finite element model

As shown in Fig. 2, the finite element software ABAQUS was used to model a simple SSPD without stiffeners. The width of the welded zone at the top and bottom of the SSPD was increased by 60 mm to avoid low cycle fatigue failure in these areas. The energy dissipation plate of the SSPD is made of 12-mm-thick low-yield steel LY 225. The energy dissipation zone is a square with a width of 200 mm. The shell element S4R, which is a 4-node general-purpose shell element with reduced integration, hourglass control, and finite membrane strains, was used to simulate the behavior of the SSPD.

For the elastic-plastic analysis, ABAQUS provides a numerical material law to simulate the behavior of metallic material under cyclic loading [17]. The kinematic hardening stress in the numerical material law can be described as

$$\alpha = \sum_{k=1}^{n} \frac{C_k}{\gamma_k}\left(1 - e^{-\gamma_k \bar{\varepsilon}^{pl}}\right) \tag{1}$$

where $\bar{\varepsilon}^{pl}$ is the EPS and C_k and γ_k are the parameters of the model. $\sigma|_0$ represents the initial yield stress. As shown in Fig. 3(a), a physical test of a common SSPD made of LYP225 was carried out. As shown in Fig. 3(b), a numerical model of the SSPD was built in ABAQUS. By using the material parameters shown in Table 1, the hysteresis curve obtained from the finite element analysis was very close to that obtained in the physical test, demonstrating the effectiveness of the material model. Therefore, the material parameters shown in Table 1 are adopted in this study. The loading scheme is shown in Fig. 4. The SPD is first loaded to an amplitude of 5 mm for three cycles, and then to an amplitude of 10 mm for three cycles, and finally to an amplitude of 20 mm for three cycles.

In the elastic-plastic analysis, EPS is sensitive to the mesh. Model verification was conducted, and three meshes with different element sizes were selected. The maximum EPS values are presented in Table. 2. Considering the balance between computational accuracy and efficiency, an element size of approximately 5 mm was chosen. The distribution of EPS in the initial model is shown in Fig. 5. It should be noticed that the acronym of Equivalent plastic strain is PEEQ in ABAQUS [17]. The EPS is concentrated in the corners of the plate, which is similar to the results presented in reference [8]. According to previous studies, the maximum plastic strain of the SSPDs has a negative relationship with the low cycle fatigue behavior [18–20]. To improve the low cycle fatigue behavior of the SSPDs, shape optimization should be carried out to reduce the maximum EPS.

3. Optimization

3.1. Optimization approach

As shown in Fig. 6, control points on the free boundary are selected to obtain the optimal shape of the energy dissipation zone. The free boundary should pass through all the control points. According to the basic theory of solid mechanics, mutation of the first derivative of the free boundary is unacceptable because of the stress concentration on

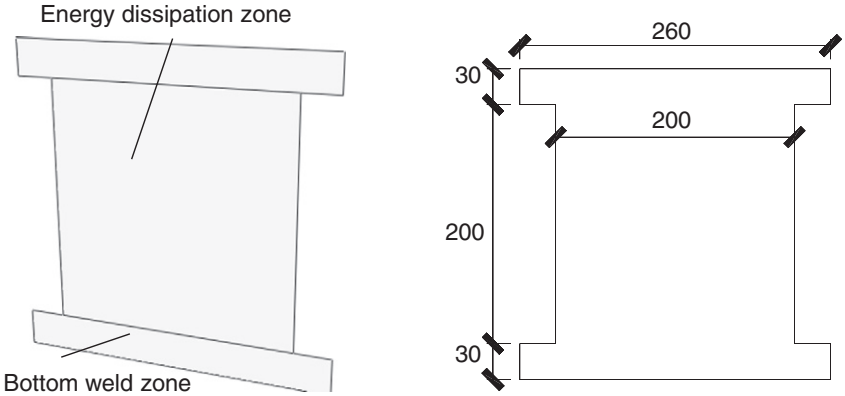

(a) 3D model (b) Dimensions of model (mm)

Fig. 2. SSPD model used in this study.

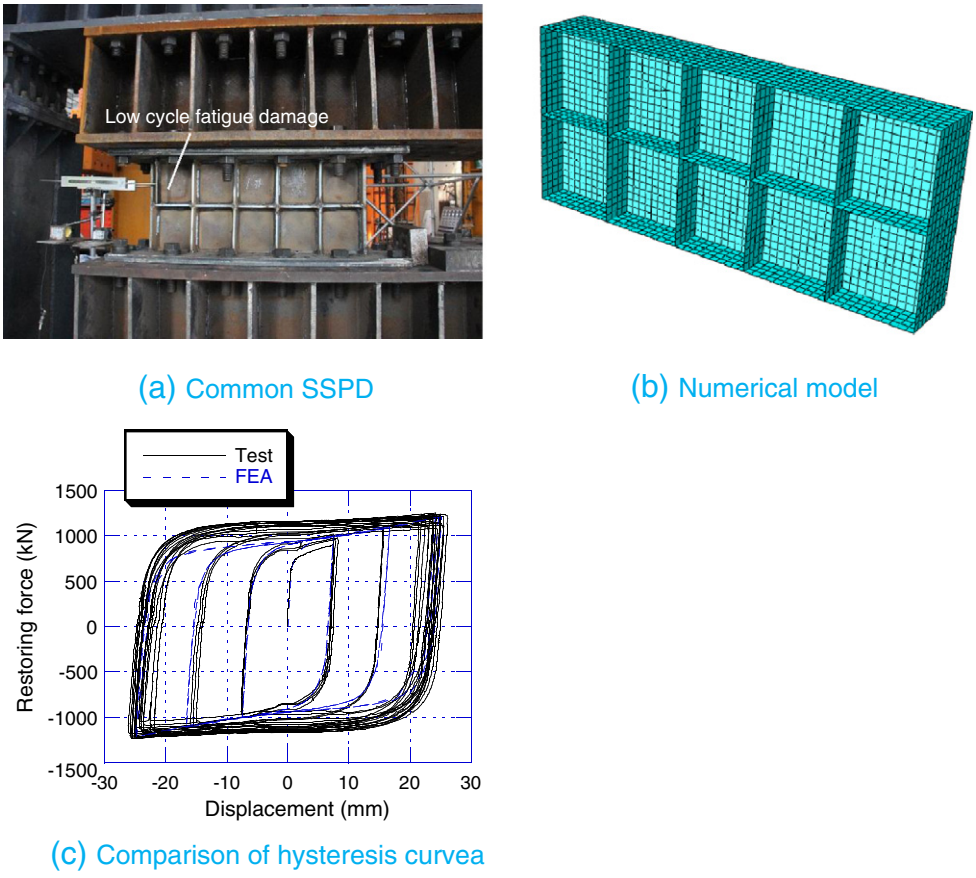

Fig. 3. Verification of numerical model.

the mutation point. The second derivative should be continuous to alleviate stress concentration [21,22]. Based on these considerations the spline function is selected, which has a continuous second derivative. According to the symmetry principle, the horizontal coordinates of the four control points, which are aligned with an interval of 20 mm in the vertical direction, are selected as the independent design variables. The optimal shape of the energy dissipation zone is equivalent to the optimal position of the control points. Four cases, where the energy dissipation zones have different aspect ratios, are considered in the shape optimization: the width of the energy dissipation zone for these cases is 150, 200, 250, and 300 mm (Fig. 6). Note that there are no constraints on the control points on the free boundary. The optimal solution obtained in this study is deemed to be the global optimal solution.

The optimization problem can be presented as Eqs. (2) and (3), where x_i denotes the variables in the optimization problem, which represents the horizontal coordinates of the control points. x_i^L and x_i^U are the lower and upper bounds of the variables, respectively. The bounds are necessary to guarantee that only reasonable models can be generated during the SA optimization process.

$$\text{Minimize} \quad PEEQ_{\max} \tag{2}$$

$$\text{subject to} \quad x_i^L \le x_i \le x_i^U \tag{3}$$

Table 1
Parameters of numerical material law (MPa).

C_1	γ_1	C_2	γ_2	C_3	γ_3	$\sigma\|_0$
20,000	400	18,000	500	1200	2	235

3.2. Optimization algorithm

With the strong material nonlinearity and geometric nonlinearity, the explicit relationship between the maximum EPS and the shape of the SSPD is difficult to derive. The traditional optimization methods, which usually require the gradient of the function, may not be able to function well to obtain the optimal solution. Therefore the simulated annealing (SA) algorithm [23] is adopted, which functions well in such a strong nonlinear optimization process. SA is an optimization algorithm categorized as a statistical heuristic search method. It is based on a local search and prevents convergence to a locally optimal solution by allowing the move to a solution that does not improve the objective function, where the probability of accepting such a solution is defined by the Metropolis criteria using the decrease (for a maximization

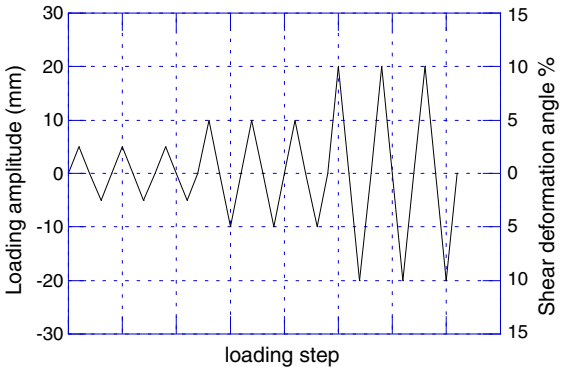

Fig. 4. Loading scheme for finite element analysis.

Table 2
Results of convergence study for FEM models.

Element size (mm)	Maximum EPS	CPU time (s)
3 mm	1.421	846.1
5 mm	0.8377	92.8
10 mm	0.5558	22.4

problem) of the objective function. The term 'simulated annealing' comes from the algorithm's ability to simulate the behavior of metals in the annealing process. Since the algorithm needs very few problem-dependent parameters, it is quite robust even for an objective function that has many local optima. MATLAB provides an optimization toolbox that uses an SA algorithm [24].

The optimization is performed by a system integrating MATLAB and ABAQUS analyses running in an iterative pattern. Fig. 7 shows the process of one iteration. First, ABAQUS/standard reads the Python script and submits the analysis job. Then the EPS is extracted by the Python script and transferred to MATLAB. MALTAB analyzes the results and updates the variables. A new model is produced by the Python script for the next round of iteration. Through many rounds of iteration, the optimal shape of the SSPDs is obtained. Note that in the process, the Python script plays an important role in the conjunction between the finite element analysis and the SA algorithm. To save computational time, the SSPD is loaded for only one cycle with an amplitude of 20 mm. The initial values of all the variables in the four cases are set to 1 mm.

3.3. Optimization results

The optimization process in Case 1 needs about 910 iterations to converge. The optimization process used about 80 h of computer time on a computer with 8 Intel Xeon CPUs and 8 GB RAM. The elastic-plastic analysis in ABAQUS accounted for about 95% of the total computational time. Because of the randomness of the SA algorithm, the number of iterations may vary for different cases. For instance, the number of iterations required to obtain the optimal solution for Case 3 was only 580. The maximum EPS values in the four optimization processes are shown in Fig. 8. After the optimization process, the maximum EPS decreased significantly. The maximum EPSs of the optimized SSPD for the four cases are about 0.3, which is much less than the maximum EPS of the initial SSPD. The optimal values of the variables are shown in Fig. 9. Note that the optimal value of the variables increased slightly when the width of the SSPD increased. The optimal shapes for the four cases and the optimal shape suggested by [8] are all shown in Fig. 10. The four optimal shapes obtained by our numerical modeling are close to each other, and the optimal shape obtained in [8] is narrower than that of Case 2.

The optimized models are loaded using the same loading scheme as the initial model described in Section 2. The EPS distributions of the optimized models and the initial models are shown in Fig. 11. Compared to the initial model, the EPS of the optimized SSPD increases in the central part of the plate while that at the corners significantly decreases. The essence of the optimization is to allow more energy dissipation in the central zone of the SSPD which results in a more uniform distribution of the plastic strain in the SSPD. The maximum EPS and energy dissipated by plastic deformation (EDPD) of the optimized and initial models are presented in Table. 3. Note that the EPSs shown in Table 3 are significantly larger than those shown in Fig. 8. This is particularly because the SSPDs are loaded for only one cycle with an amplitude of 20 mm when obtaining the optimal shapes, while they are loaded for 3 cycles with amplitudes of 5 mm, 10 mm and 20 mm, respectively when comparing optimized models to initial models. The maximum EPS values in the four cases are very close and are not dependent on the width of the SSPD. The maximum EPS is significantly decreased to about one-third of the initial model EPS. On the other hand, the EDPD remains about 90% of that of the initial model. This demonstrates the effectiveness of the shape optimization in improving the low cycle fatigue performance of the SSPD.

Fig. 12 shows the optimal shape obtained in Case 2 and the optimal shape suggested by reference [8]. The distribution of the EPS in the optimal model of Case 2 is more uniform than that obtained in reference [8]. The central zone in our model provides more energy dissipation capacity. The maximum EPS of the SSPD with the global optimal shape is 1.615 less than the value of the SSPD with the local optimal shape. The EDPDs of the two models shown in Fig. 12 are 99.10 kN m and 111.44 kN m, respectively, demonstrating the improved energy dissipation capacity of the global optimal solution over the local optimal solution.

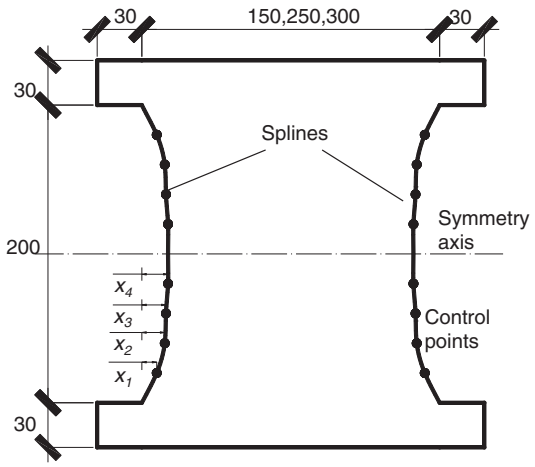

Fig. 6. SSPD model used in optimization.

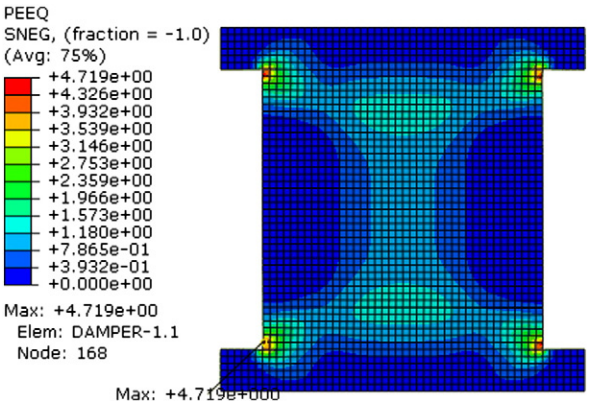

Fig. 5. Distribution of EPS for Case 2.

4. Conclusions

Shape optimization of SSPDs was carried out to improve their low cycle fatigue behavior. The numerical model was incorporated in the finite element software ABAQUS. A simulated annealing algorithm, which is suitable for solving strong nonlinear optimization problems, was adopted for the optimization. Finally, the optimal shape for various

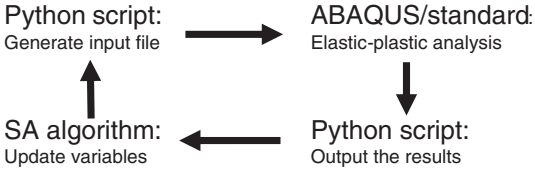

Fig. 7. Optimization flow chart.

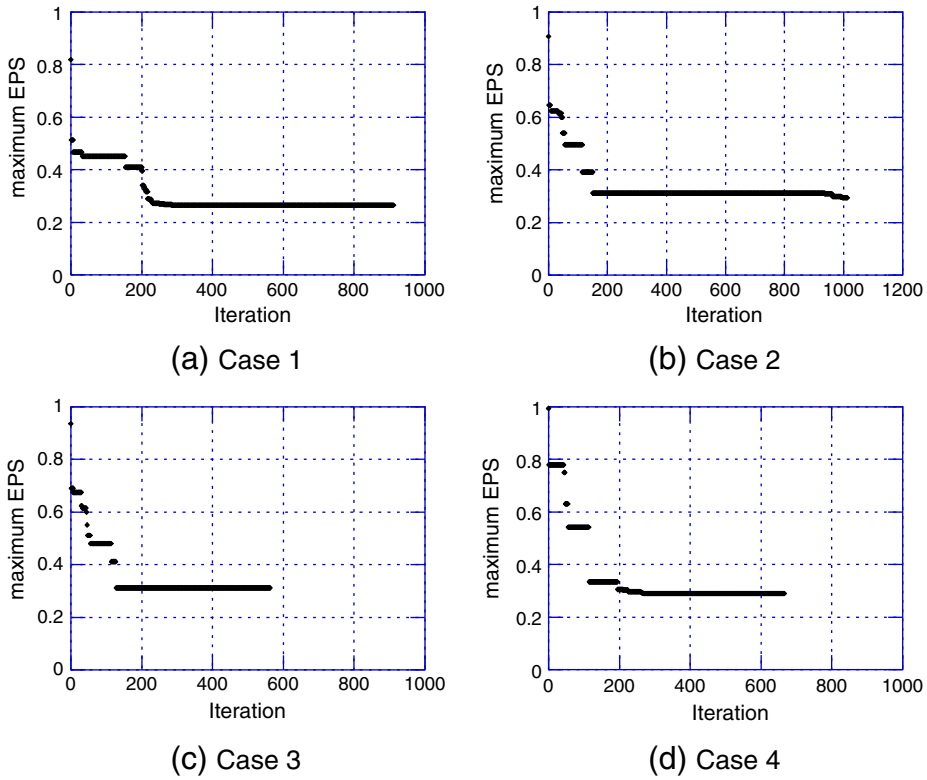

Fig. 8. Maximum EPS values obtained in the optimization process for Cases 1–4.

sizes of SSPD was derived. The major conclusions in the research are as follow:

1) The optimal shape of the SSPD can be obtained by an SA algorithm in conjunction with finite element software.
2) The global optimal solution shows better performance than the local optimal solution with a parabolic free boundary constraint.
3) The low cycle fatigue performance of the SSPD can be significantly improved by the shape optimization. The maximum EPS of the optimized SSPD is only one third than that of the conventional SSPD for a cyclic loading scheme.
4) SSPDs with optimized shape have a much better low cycle fatigue performance but show only a small decrease in their energy dissipation capacity.

Acknowledgments

The authors gratefully acknowledge the financial support from the "Twelfth Five-Year" plan major projects supported by the National Science and Technology of China under grant no. 2012BAJ07B02, the Natural Science Foundation of China under grant nos. 51178250, 51261120377, and 91315301, and the Tsinghua University Initiative Scientific Research Program under grant nos. 2012THZ07 and 2010Z01001.

References

[1] Pan P, Ye LP, Shi W, et al. Engineering practice of seismic isolation and energy dissipation structures in China [J]. Sci China Technol Sci 2012;55(11):3036–46.

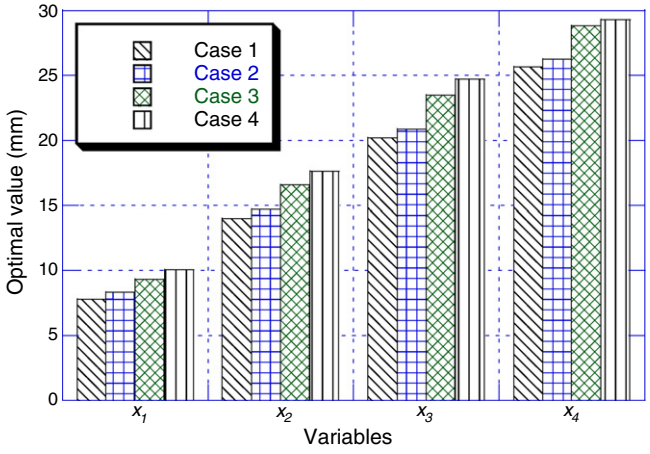

Fig. 9. Optimization values of variables.

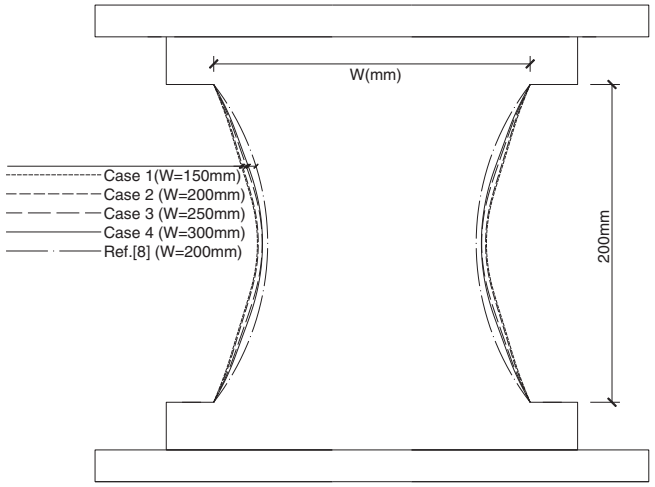

Fig. 10. Optimal plate shapes for Case 1–4 and that of Liu and Shimoda [8].

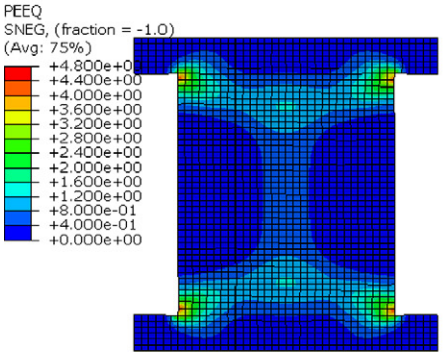

(a) Initial shape in Case 1

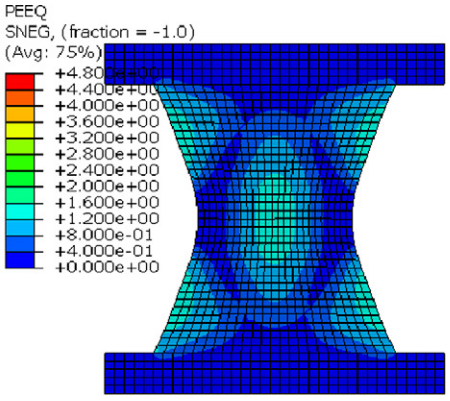

(b) Optimal shape in Case 1

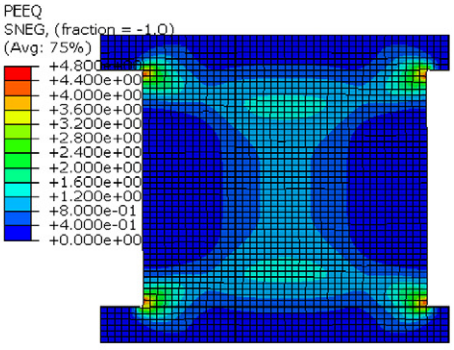

(c) Initial shape in Case 2

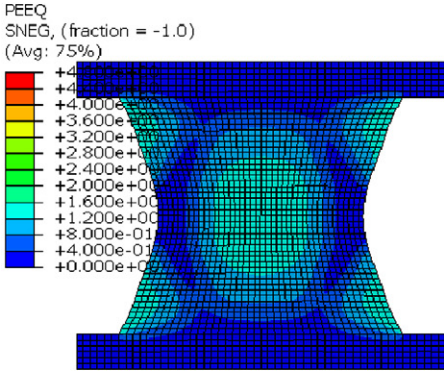

(d) Optimal shape in Case 2

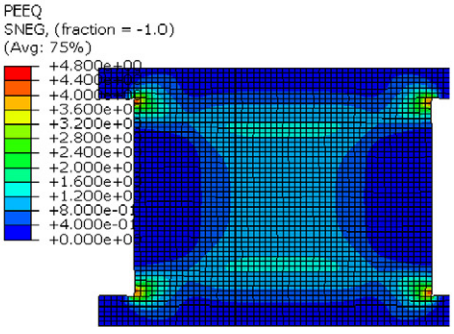

(e) Initial shape in Case 3

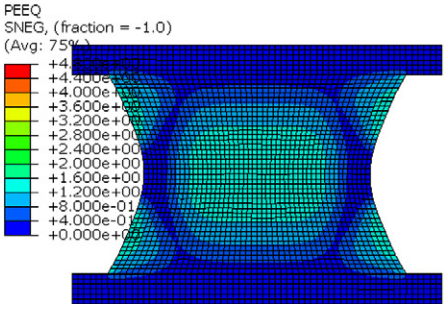

(f) Optimal shape in Case 3

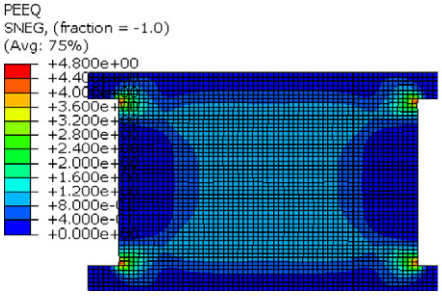

(g) Initial shape in Case 4

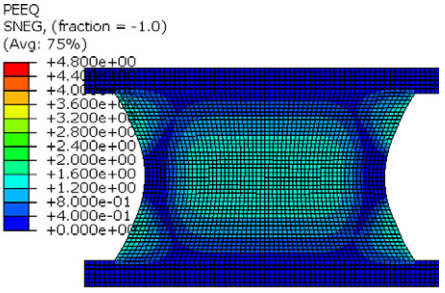

(h) Optimal shape in Case 4

Fig. 11. EPS distribution of initial and optimized models.

Table 3
Comparison between initial and optimal models.

Case	Initial model		Optimized model	
	EPS	EDPD (kN m)	EPS	EDPD (kN m)
No. 1 (150 mm)	4.717	80.74	1.473	69.70
No. 2 (200 mm)	4.719	123.12	1.615	111.30
No. 3 (250 mm)	4.719	165.40	1.641	151.85
No. 4 (300 mm)	4.738	208.23	1.561	193.46

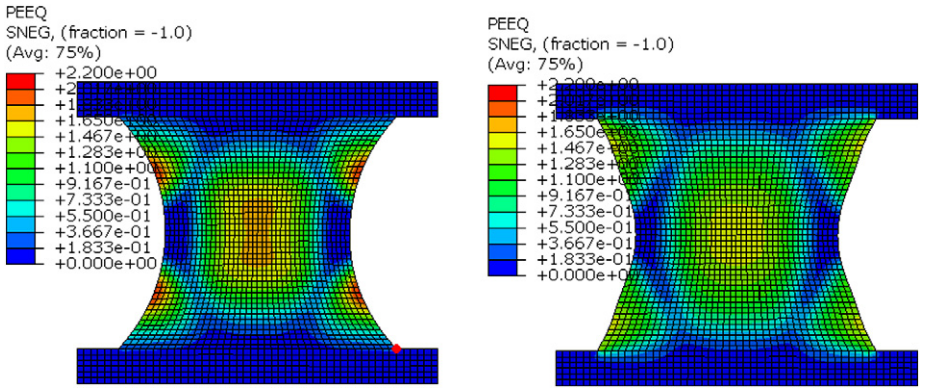

(a) Suggested by reference [8] (maximum EPS: 2.172 EDPD: 99.10kN*m)

(b) Optimal solution of Case 2 (maximum EPS:1.615 EDPD: 111.30kN*m)

Fig. 12. Comparison between optimal solutions of reference [8] and this study.

[2] Soong TT, Spencer Jr BF. Supplemental energy dissipation: state-of-the-art and state-of-the-practice [J]. Eng Struct 2002;24(3):243–59.
[3] Skinner RI, Kelly JM, Heine AJ. Hysteretic dampers for earthquake resistant structures [J]. Earthq Eng Struct Dyn 1974;3(3):287–96.
[4] De Matteis G, Landolfo R, Mazzolani FM. Seismic response of MR steel frames with low-yield steel shear panels [J]. Eng Struct 2003;25(2):155–68.
[5] Chan RWK, Albermani F. Experimental study of steel slit damper for passive energy dissipation [J]. Eng Struct 2008;30(4):1058–66.
[6] Radaj D. Heat effects of welding: temperature field, residual stress, distortion [M]. New York: Springer; 1992.
[7] Sonsino CM. Effect of residual stresses on the fatigue behaviour of welded joints depending on loading conditions and weld geometry [J]. Int J Fatigue 2009;31(1):88–101.
[8] Zhang C, Zhang Z, Shi J. Development of high deformation capacity low yield strength steel shear panel damper [J]. J Constr Steel Res 2012;75:116–30.
[9] Liu Y, Aoki T, Shimoda M. Strain distribution measurement of a shear panel damper developed for bridge structure [J]. J Struct 2013:1–11.
[10] Liu Y, Shimoda M. Shape optimization of shear panel damper for improving the deformation ability under cyclic loading [J]. Structural and Multidisciplinary Optimization; 2013 1–9.
[11] Ohsaki M. Optimization of finite dimensional structures [M]. CRC Press; 2010.
[12] Pan P, Ohsaki M, Tagawa H. Shape optimization of H-beam flange for maximum plastic energy dissipation [J]. J Struct Eng 2007;133(8):1176–9.
[13] Goldberg DE. Genetic algorithms in search, optimization and machine learning. Addison Wesley; 1989.
[14] Xu YH, Li AQ, Zhou XD, et al. Shape optimization study of mild steel slit dampers [J]. Adv Mater Res 2011;168:2434–8.
[15] Vanderplaats GN. Multidiscipline design optimization. Vanderplaatz R&D Inc.; 2007.
[16] Ohsaki M, Nakajima T. Optimization of link member of eccentrically braced frames for maximum energy dissipation [J]. J Constr Steel Res 2012;75:38–44.
[17] Version A. 6.10 EF1 user manual. ABAQUS [J]; 2011.
[18] Manson SS. Discussion. Trans ASME 1962;84:537–41.
[19] Coffin Jr LF. A study of the effects of cyclic thermal stresses on a ductile metal. Trans ASME 1954;76:931–50.
[20] Deng K, Pan P, Wang C. Development of crawler steel damper for bridges [J]. J Constr Steel Res 2013;85:140–50.
[21] Niu Q, Shephard MS. Super-convergent extraction techniques for finite element analysis [J]. Int J Numer Methods Eng 1993;36(5):811–36.
[22] Niu Q, Shephard MS. Super-convergent boundary stress extraction and some experiments with adaptive point wise error control [J]. Int J Numer Methods Eng 1994;37(5):877–91.
[23] Goffe WL, Ferrier GD, Rogers J. Global optimization of statistical functions with simulated annealing [J]. J Econom 1994;60(1):65–99.
[24] Toolbox O. user's guide. Natick, MA, USA: The MathWorks [J]. Inc.; 2010.